Transverse-Flow Gas Lens

Harold Mirels,* Donald J. Spencer,† and Robert Hofland‡
The Aerospace Corporation, El Segundo, California 90245

The concept of a transverse-flow gas lens is described. In this device, gas flows between two parallel plates that are heated or cooled so as to generate a parabolic variation of index of refraction in the region between the plates. A laser beam, propagating normal to the gas flow, can then be diverged, converged, or focused. A single module acts like a cylindrical lens. The use of two or three modules, arranged in an orthogonal manner, provides a spherical lens. Equations and tables are provided for the design of one-, two-, and three-module configurations. The advantages of the transverse-flow gas lens (relative to a device with a flow along the optic axis) are 1) thermal blooming is minimized (due to short residence time of fluid in laser beam); 2) the index of refraction profile is the same throughout each module, leading to good beam quality; and 3) the system is readily scaleable. However, a longer distance along the optical axis may be needed by the transverse-flow lens.

Introduction

IT is known that gases transported within a tube can act to diverge, collimate, or focus a beam of light directed along the axis of the tube. It is also known that high-intensity laser light can damage solid lenses. Thus, a lens constructed using a gas flow with low light absorption is of interest because of its ability to accommodate high light intensities that would otherwise damage solid lenses.

A pipe-flow gas lens concept has been proposed by Marcuse and Miller.[1] In this concept, a laser beam is propagated through a cooled rotating pipe that confines a relatively warm flowing gas (Fig. 1a). A shown in Fig. 1b, the radial temperature variation of the gas flowing in the pipe produces a radial refractive index variation that corresponds to a negative optical lens. The use of a warm pipe and a relatively cool gas, as discussed in Ref. 1, produces a positive optical lens. A more recent discussion of the performance of the pipe-flow gas lens, as well as its application as a defocusing optical element in free electron lasers, has been given by Christiansen.[2]

There are several shortcomings associated with the pipe-flow gas lens concept. First, the radial variation of the index of refraction is not parabolic in the pipe inlet boundary-layer region. This nonparabolic index variation may produce aberrations that degrade beam quality. Second, at high optical intensities, these devices are susceptible to distortions caused by the heating of the gas and thermal blooming because of the long dwell time of the gas in the laser-beam path. The amount of distortion increases as the beam travels along the optic axis. Third, these devices are not scaleable because optical power is reduced in the downstream flow region due to gas-wall temperature equilibration, as indicated in Fig. 1b.

These limitations can be circumvented by the use of a gas flow that is transverse rather than parallel to the optical axis. This concept, termed a transverse-flow gas lens, is illustrated in Figs. 2-5 for the case of a negative optical lens (i.e., cooled wall) which is of interest as a beam diverging element in a free electron laser.[2] A high-quality gas lens module, for control of a laser beam, can be established by generating a fully developed thermal boundary-layer gas flow between two cooled parallel plates as indicated in Fig. 2a. When a laser beam is propagated transverse to the flow direction, in the fully developed thermal boundary-layer region, a cylindrical divergence of the beam is produced, as shown in Fig. 2b. Two such modules, mounted in line with the laser-beam path and with gas flow directions orthogonal to one another, provide an exit beam with a spherical wave front and an elliptical cross section as shown in Fig. 3. As shown in Fig. 4, three modules can be mounted in line to generate an exit beam with a spherical wave front and a circular cross section, functioning as a single spherical diverging lens. The array depicted in Fig. 4 is a three module system in which the central module, operating on the z-beam component, is sandwiched between and orthogonal to the two bookend modules that operate on the y-beam component. A schematic representation of optical ray paths through a three-module system is shown in Fig. 5.

In the present paper, we discuss the performance of a transverse-flow gas lens. Thermal boundary-layer development, index of refraction profiles, and optical ray paths are discussed. Designs of one-, two-, and three-module systems are then noted.

Theory

Thermal Boundary Layer

The thermal boundary-layer development is assumed to consist of an inlet region and a fully developed flow region, as

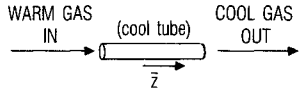

a) Configuration of Ref. 1

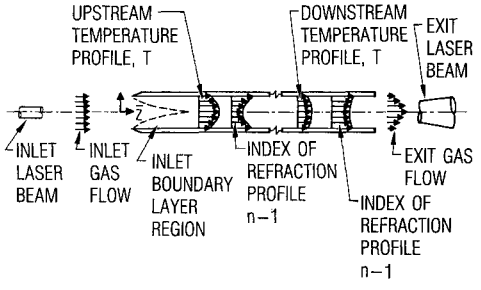

b) Temperature and index of refraction profiles

Fig. 1 Schematic diagram of a pipe flow gas lens.[1] A negative (divergent) lens is illustrated.

Presented as Paper 89-1907 at the AIAA 20th Fluid Dynamics, Plasma Dynamics and Lasers Conference, Buffalo, NY, June 12-14, 1989; received Oct. 10, 1989; revision received May 22, 1990; accepted for publication May 24, 1990.

*Principal Scientist, Aerophysics Laboratory, 2350 East El Segundo Blvd. Fellow AIAA.

†Senior Scientist, Aerophysics Laboratory, 2350 East El Segundo Blvd. Member AIAA.

‡Head, Laser Physics Department, Aerophysics Laboratory, 2350 East El Segundo Blvd. Member AIAA.

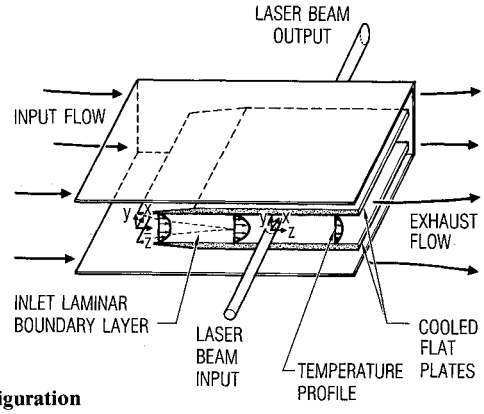

a) Configuration

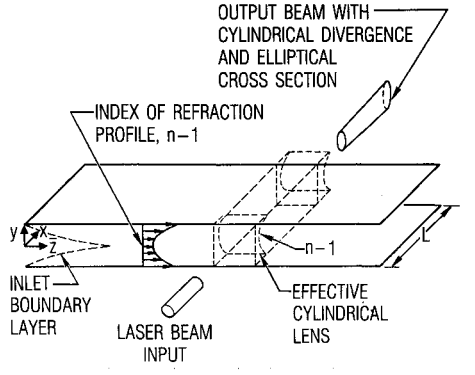

b) Effective cylindrical lens

Fig. 2 Schematic diagram of one module of a transverse-flow gas lens. For the case of a collimated input beam with circular cross section, this configuration provides an exit beam with cylindrical divergence and elliptical cross section.

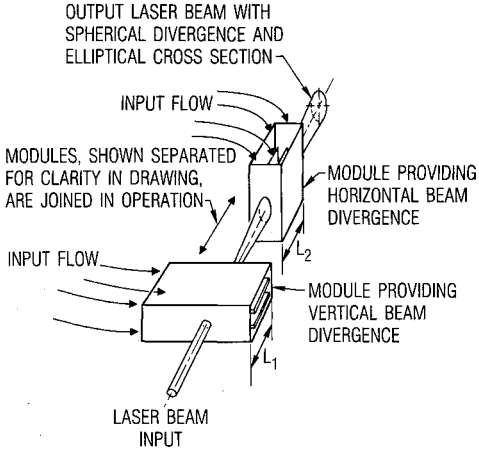

Fig. 3 Schematic diagram of two orthogonal modules of a transverse-flow gas lens. For the case of a collimated input beam with circular cross section, these modules provide an exit beam with spherical divergence and elliptical cross section.

illustrated in Fig. 6. The thermal boundary-layer growth in the inlet region is estimated using the conventional semi-infinite laminar flat-plate expression. Thus, the thermal boundary-layer growth along the flow direction is described approximately by

$$\delta_{th} = 5(\mu\bar{z}/\rho v)^{1/2}Pr^{-1/3} \tag{1}$$

where $\bar{z}$ denotes streamwise distance measured from the leading edge of the cooled plate; δ_{th} is the thermal boundary-layer thickness; v is the gas velocity in the streamwise direction; μ, k, ρ, and C_p are the gas viscosity, thermal conductivity, density, and heat capacity; and $Pr = \mu C_p/k$ is the gas Prandtl number. The latter gas properties are based on the average boundary-layer temperature. Thermal boundary-layer development is shown schematically by the dashed curve in Fig. 6. Typical values of flow parameters are included in Fig. 6 for the case of an argon gas and walls cooled by liquid oxygen.

Boundary-layer closure occurs when $2\delta_{th} = D$, where D is the plate separation distance. The corresponding streamwise location is denoted $\bar{z}_c$ and is found from

$$\bar{z}_c/v = (D^2/100)(\rho/\mu)(Pr)^{2/3} \tag{2}$$

Note that for fixed D and gas properties, $\bar{z}_c$ varies linearly with v. It is necessary that the flow remains laminar upstream of the closure region in order to assure an optical medium with good beam quality. A criterion for laminar flow in this region is

$$Re_c \equiv \rho v\bar{z}_c/\mu \equiv [(\rho vD)/10\mu)]^2Pr^{2/3} \leq 10^5$$

where Re_c is the Reynolds number based on inlet length $\bar{z}_c$.

Downstream of the boundary-layer closure region, the fluid temperature profile may be approximated by

$$\frac{T_0 - T}{T_0 - T_w} = (2y/D)^2 \tag{3}$$

where T_0 and T_w denote local centerline and local wall temperatures, respectively, and y denotes lateral distance from the centerline. The variation of index of refraction with gas properties is given by an expression in Table 1. Assuming an ideal gas and a negligible pressure variation in the y direction, the corresponding index of refraction variation is

$$\frac{n - n_0}{n_w - n_0} = (2y/D)^2(T_w/T) \tag{4}$$

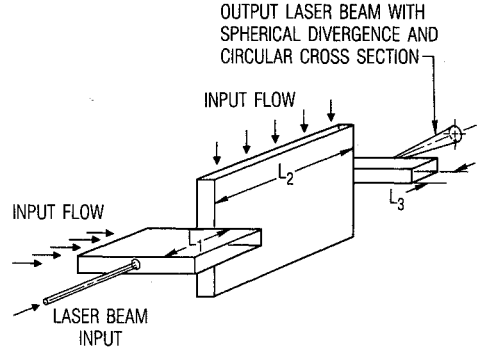

Fig. 4 Schematic diagram of a three-module transverse-flow gas lens. For the case of a collimated input beam with circular cross section, this configuration provides an exit beam with spherical divergence and circular cross section.

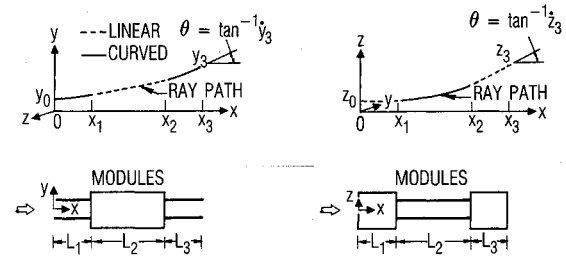

a) End view b) Bottom view

Fig. 5 Ray paths through orthogonal components of a three-module transverse-flow gas lens.

Table 1 Index of refraction for various gases at wavelength $\lambda = 5893$ Å

Gas	Air	N_2	CO_2	Ar	He
$\beta \times 10^4$	2.9	3.0	4.5	2.8	0.36

$n - 1 = \beta \times P(\text{atm})\ [273/T°(K)]$.

Table 2 Values that allow the design of a single-module transverse-flow gas lens with a cylindrical output beam

$\dot{y}_1/(A_1 y_0)$	y_1/y_0	$A_1 L_1$	$1/(A_1 R)$
0.000	1.000	0.000	0.000
0.100	1.005	0.100	0.100
0.200	1.020	0.199	0.196
0.400	1.077	0.390	0.371
0.600	1.166	0.569	0.514
0.800	1.281	0.733	0.625
1.000	1.414	0.881	0.707
2.000	2.236	1.444	0.894
3.000	3.162	1.818	0.949

An optical beam, of diameter $d \ll D$, which propagates in the x direction, encounters an essentially parabolic index variation given by

$$\frac{n - n_0}{n_w - n_0} = \left(\frac{2y}{D}\right)^2 \frac{T_w}{T_0}\left[1 + 0\left(1 - \frac{T_w}{T_0}\right)\left(\frac{d}{D}\right)^2\right] \tag{5}$$

The index variation in Eq. (5) is equivalent to a diverging cylindrical lens when $T_w < T_0$ (i.e., $n_w > n_0$) and is equivalent to a converging cylindrical lens when $T_w > T_0$ (i.e., $n_w < n_0$). The optical performance of these lenses is described in the next section.

Optical Performance

We consider multiple-module configurations, wherein the laser beam propagates in the x direction. The beam entrance and exit station for the ith module is denoted x_{i-1} and x_i, respectively, and the length of each module, in the beam direction, is $L_i = x_i - x_{i-1}$ (Fig. 5).

We first consider modules where the flow is in the $\bar{z}$ direction and denote downstream distance, measured from the beam centerline, by z (Fig. 2a). We assure a parabolic index variation in the y direction and a negligible index variation in the z direction. These conditions apply for modules 1 and 3 in Fig. 5. The variation of ray ordinates y and z with distance along the beam is, in general,[4]

$$\frac{\partial^2 y}{\partial x^2} = \frac{\partial n}{\partial y} \tag{6a}$$

$$\frac{\partial^2 z}{\partial x^2} = \frac{\partial n}{\partial z} \tag{6b}$$

For the parabolic index variation in the y direction [given by Eq. (5)] and no index variation in the z direction, Eq. (6) becomes

$$\frac{\partial^2 y}{\partial x^2} = A_i^2 y \tag{7a}$$

$$\frac{\partial z}{\partial x} = 0 \tag{7b}$$

where

$$A_i^2 = [8(T_w/T_0)(n_w - n_0)/D^2]_i \tag{7c}$$

Note that A_i is real for $n_w > n_0$, which is the case of primary interest, and A_i is imaginary for $n_w < n_0$. Let y_{i-1}, z_{i-1} and y_i, z_i denote beam ordinates at the entrance and exit of the ith module, respectively. Integration of Eq. (7a) for A_i real yields

$$y_i = y_{i-1} \cosh A_i L_i + [(\dot{y}_{i-1})/A_i] \sinh A_i L_i \tag{8a}$$

$$\dot{y}_i = A_i y_{i-1} \sinh A_i L_i + \dot{y}_{i-1} \cosh A_i L_i \tag{8b}$$

When A_i is imaginary, the hyperbolic functions in Eqs. (8a) and (8b) are replaced by the corresponding trigonometric functions of $|A_i| L_i$. Integration of Eq. (7b) yields

$$z_i = z_{i-1} + \dot{z}_{i-1} L_i \tag{8c}$$

$$\dot{z}_i = \dot{z}_{i-1} \tag{8d}$$

which represents a linear variation.

The ordinates y and z are reversed in Eqs. (7) and (8) for modules with a parabolic index variation in the z direction and no index variation in the y direction (e.g., module 2 in Fig. 5).

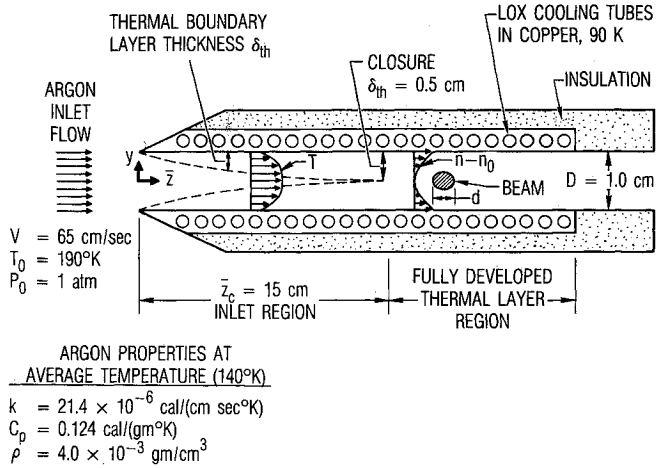

Fig. 6 Schematic diagram showing thermal boundary-layer growth between two cooled plates.

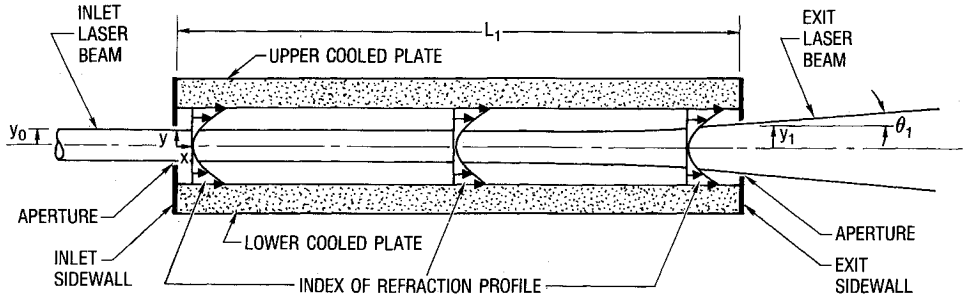

Fig. 7 Schematic diagram showing laser-beam path within first module.

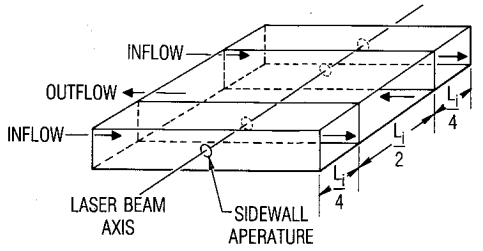

Fig. 8 Schematic diagram that indicates the use of counterflow to compensate for a linear streamwise variation of index of refraction. A single module is shown. The central section has twice the width of the two end sections.

These expressions are used in the following sections to obtain the performance of gas lenses with one, two, or three modules.

One-Module Configuration

A single module with flow in the z direction, beam propagation in the x direction, and a parabolic index variation in the y direction is illustrated in Figs. 2 and 7. For the case of a collimated input beam, inlet and exit ordinates are related by $z_1 = z_0$, $\dot{z}_1 = \dot{z}_0 = 0$ and

$$y_1/y_0 = \cosh(L_1A_1) \tag{9a}$$

$$\dot{y}_1/(A_1y_0) = \sinh(L_1A_1) \tag{9b}$$

The output beam has a cylindrical wave front of radius R given by

$$\frac{1 + 0(y_1/R)^2}{R} = \frac{\dot{y}_1}{y_1} = A_1 \tanh(A_1L_1) \tag{9c}$$

where terms of order $(y_1/R)^2$ have been neglected. Thus, the module functions like a cylindrical lens. An input beam with a circular cross section will have an elliptical cross section, with a ratio of major to minor axis equal to $\cosh L_1A_1$, at the exit of the module. In the limit $A_1L_1 \to 0$, Eqs. (9) become $y_1 = y_0$ and

$$\frac{\dot{y}_1}{A_1y_0} = \frac{1}{A_1R} = A_1L_1[1 + 0(A_1L_1)^2] \tag{10}$$

which is a thin lens approximation for module performance.

Equations (9) have been evaluated for $0.0 \le \dot{y}_1/A_1y_0 \le 3.0$. The corresponding results for y_1/y_0, A_1L_1, and $1/A_1R$ are given in Table 2. These results also apply for the case of a pipe-flow configuration (Fig. 1) if it is assumed that A_1 is constant along the optical axis. Table 2 can then be used to compare the length of a pipe-flow configuration with the length of an equivalent multiple-module transverse-flow lens designed to provide a spherically divergent output beam.

Two-Module Configuration

For the case of two modules with a collimated inlet beam, as indicated in Fig. 3, inlet and exit beam properties are related by

$$y_2/y_0 = \cosh A_1L_1 + A_2L_2(A_1/A_2)\sinh A_1L_1 \tag{11a}$$

$$\dot{y}_2/(A_2y_0) = (A_1/A_2)\sinh A_1L_1 \tag{11b}$$

$$z_2/z_0 = \cosh A_2L_2 \tag{11c}$$

$$\dot{z}_2/(A_2z_0) = \sinh A_2L_2 \tag{11d}$$

The exit beam will have a spherical wave front of radius R if

$$\frac{1}{R} = \frac{\dot{y}_2}{y_2} = \frac{\dot{z}_2}{z_2} \tag{12}$$

where terms of order $(y_2/R)^2$ and $(z_2/R)^2$ are neglected. If the inlet beam has a circular cross section, the exit beam will have an elliptical cross section with the ratio of major to minor axis equal to y_2/z_2. If A_1, A_2, and R are specified, Eq. (12) provides two equations for L_1 and L_2. Other properties are found from Eqs. (11). For the case $A_1 = A_2 \equiv A$, it is found that

$$AL_2 = \coth^{-1}(AR) \tag{13a}$$

$$AL_1 = \coth^{-1}(AR - AL_2) \tag{13b}$$

Numerical results for this case are given in Table 3. These results were obtained by specifying $\dot{z}_2/(Az_2)$ and obtaining AL_2 from Eq. (11d). Other variables were then obtained from Eqs. (11-13). Equation (13b) requires $A(R - L_2) \ge 1$, which results in the requirements $AR \ge 1.6837$, $AL_2 \le 0.6837$, and $AL_1 \le 5.5520$. It follows that $\dot{z}_2/(Az_2) \le 0.7383$, $z_2/z_0 \le 1.2430$, $\dot{y}_2/(Ay_2) \le 128.87$, and $y_2/y_0 \le 216.98$. These limitations do not affect the ability to design a two-module gas lens since the quantity A is a design variable. The larger the value of A, the smaller the values of L_1 and L_2 required to achieve a given divergence and the more nearly each module acts like a thin (rather than a thick) lens.

Tables 2 and 3 permit a comparison of the lengths required to achieve a given spherical divergence in a pipe-flow lens (Table 2) and in a two-module transverse-flow lens (Table 3). For a given value of A, the latter requires approximately twice the length of the former. This is due to the fact that the pipe-flow lens provides a spherical divergence at each flow station, whereas the transverse-flow gas lens requires a sequence of two cylindrical expansions to achieve a spherical output. A more accurate length comparison requires consideration of achievable values of A in each device and consideration of the variation of A along the optical axis in the pipe-flow device.

Table 3 Values that allow the design of a two-module transverse-flow gas lens with spherical wave front and elliptical cross-section output

$\dot{z}_2/(Az_0)$	z_2/z_0	$\dot{y}_2/(Ay_0)$	y_2/y_0	AL_1	AL_2	$A(L_1+L_2)$	$1/(AR)$	$(y_2/z_2)-1$
0.000	1.000	0.000	1.000	0.000	0.000	0.000	0.000	0.000
0.100	1.005	0.101	1.015	0.101	0.100	0.201	0.100	0.010
0.200	1.020	0.208	1.063	0.207	0.199	0.406	0.196	0.042
0.300	1.044	0.331	1.151	0.325	0.296	0.621	0.287	0.103
0.400	1.077	0.482	1.298	0.465	0.390	0.855	0.371	0.205
0.500	1.118	0.693	1.551	0.647	0.481	1.129	0.447	0.387
0.600	1.166	1.060	2.060	0.923	0.569	1.492	0.514	0.767
0.700	1.221	2.291	3.995	1.567	0.653	2.219	0.573	2.273
0.710	1.226	2.697	4.659	1.718	0.661	2.379	0.579	2.799
0.720	1.232	3.396	5.811	1.937	0.669	2.606	0.584	3.716
0.730	1.238	5.111	8.668	2.334	0.677	3.011	0.590	6.001
0.738	1.243	30.381	51.164	4.107	0.684	4.791	0.594	40.167

Table 4 Values that allow the design of a three-module transverse-flow gas lens with spherical wave front and circular cross-section output

$\dot{r}_3/(Ar_0)$	r_3/r_0	AL_1	AL_2	AL_3	$A(L_1+L_2+L_3)$	$1/(AR)$
0.000	1.000	0.000	0.000	0.000	0.000	0.000
0.200	1.039	0.099	0.199	0.097	0.395	0.192
0.400	1.150	0.195	0.390	0.182	0.767	0.348
0.600	1.315	0.285	0.569	0.248	1.102	0.456
0.800	1.519	0.369	0.733	0.298	1.399	0.527
1.000	1.749	0.446	0.881	0.335	1.661	0.572
1.200	1.997	0.517	1.016	0.362	1.895	0.601
1.400	2.258	0.583	1.138	0.384	2.104	0.620
1.600	2.528	0.644	1.249	0.401	2.294	0.633
1.800	2.806	0.701	1.350	0.415	2.466	0.642
2.000	3.088	0.755	1.444	0.426	2.624	0.648
2.200	3.375	0.805	1.530	0.436	2.770	0.652
2.400	3.665	0.853	1.609	0.444	2.906	0.655
2.600	3.958	0.898	1.684	0.451	3.032	0.657
2.800	4.253	0.941	1.753	0.457	3.151	0.658
3.000	4.550	0.982	1.818	0.462	3.262	0.659
100.000	158.373	3.677	5.298	0.584	9.559	0.631

Three-Module Configuration

In the case of three modules with a collimated inlet beam, as in Fig. 4, inlet and exit beam properties are related by

$$y_3/y_0 = [\cosh A_1L_1 + (A_2L_2)(A_1/A_2)\sinh A_1L_1]\cosh A_3L_3 + (A_1/A_3)\sinh A_1L_1 \sinh A_3L_3 \quad (14a)$$

$$\dot{y}_3/(A_3y_0) = [\cosh A_1L_1 + L_2A_2(A_1/A_2)\sinh A_1L_1]\sinh A_3L_3 + (A_1/A_3)\sinh A_1L_1 \cosh A_3L_3 \quad (14b)$$

$$z_3/z_0 = \cosh A_2L_2 + A_3L_3(A_2/A_3)\sinh A_2L_2 \quad (14c)$$

$$\dot{z}_3/(A_3z_0) = (A_2/A_3)\sinh A_2L_2 \quad (14d)$$

The exit beam will have a spherical wave front of radius R if

$$\frac{1}{R} = \frac{\dot{y}_3}{y_3} = \frac{\dot{z}_3}{z_3} \quad (15a)$$

If the input beam is circular, the exit beam will have a circular cross section provided

$$\frac{y_3}{y_0} = \frac{z_3}{z_0} \quad (15b)$$

When R, A_1, A_2, and A_3 are specified, Eqs. (15) provide three equations for L_1, L_2, and L_3. The solution of these equations is simplified if the practical assumption $A_1 = A_1 = A_3 = A$ is made. Numerical results for this case are given in Table 4. These results were obtained by specifying

$$\dot{y}_3/(Ay_0) = \dot{z}_3/(Az_0) \equiv \dot{r}_3/(Ar_0)$$

obtaining AL_2 from Eq. (14d) and then obtaining the remaining variables from Eqs. (14) and (15). There does not appear to be a mathematical limitation on allowed values for $\dot{r}_3/(Ay_0)$. For small exit values of $\dot{y}/(Ay_0)$ and $\dot{z}/(Az_0)$, the two- and three-module transverse-flow gas lens configurations give similar performance. In these cases, the two-module configuration is simpler and is preferable. With increase in exit divergence, the overall length of the three-module system is less than that of the two-module system for a given value of A. Moreover, the three-module system provides an exit beam with a circular cross section.

For small exit divergence angles, AL_1 and AL_2 in the two-module configuration equal, respectively, $AL_1 + AL_3$ and AL_2 in the three-module configuration. Hence, the first module in the former is split into two halves in the latter. The net length of the two- and three-module device is the same. With increase in exit divergence angles, the net length of the three-module device tends to become smaller than that of the two-module device as previously noted.

Compensation for Streamwise Index Variation

The effect of a streamwise variation of the index of refraction has been neglected [e.g., Eq. (7b)]. The latter variation can be caused by wall shear-induced pressure gradient, by wall heat-transfer-induced centerline temperature gradient, and by laser heating of the flowing gas. A linear streamwise index of refraction variation acts like an optical wedge and tends to tilt the laser beam. This effect can be compensated for by the subdivision of each module into three sections with counterflow in the central section, as indicated in Fig. 8. The width of the central section is twice the width of each end section. In principle, the configuration in Fig. 8 provides an exact compensation for a linear streamwise variation in refractive index. It is preferable, however, to avoid significant streamwise gradients by appropriate choice of flow variables.

Concluding Remarks

Each module requires at least two sidewalls (e.g., Fig. 7). For a high power laser beam, each sidewall may require an aperture to allow transit of the laser beam. The sidewalls and apertures are potential sources of beam quality degradation. This degradation can be minimized by the following: 1) use of thermal insulator sidewall material so as to minimize the sidewall impact on the gas flow temperature profile, 2) use of small sidewall aperture diameters, and 3) use of low values of the design parameter A so as to increase the optical path length within each module and thereby reduce the relative importance of the aperture region.

The transverse-flow gas lens concept has been described in terms of cooled plates to produce beam divergence. The use of heated plates will produce a reversal in the gas flow temperature gradients and a resultant positive lens. The latter may be used for collimating a diverging beam or for focusing. When $T_w > T_0$, the parameter A_i is imaginary [Eq. (7c)] and the hyperbolic functions are replaced by trigonometric functions in Eqs. (8–14), as previously noted.

Finally, it should be noted that the transverse-flow gas lens concept requires only that the index of refraction profile be parabolic in the vicinity of the channel centerline [e.g., $(n-n_0)_i = (A_i^2/2)y^2$]. This condition is automatically satisfied, in a fully developed flow, if the origin of the y-coordinate system is taken to be the plane where the gas temperature is a maximum (for a negative lens) or a minimum (for a positive lens). The origin is offset from the channel centerline when the wall temperatures differ. The expression for A_i in Eq. (7c) may be viewed as approximate in view of the approximate nature of Eq. (3). However, the parametric dependence of A_i^2 on $(T_w/T_0)(n_w - n_0)/D^2$, indicated in Eq. (7c), is basically correct. Small variations of this parameter permit fine-tuning of an experimental device to achieve any desired performance.

References

[1]Marcuse, D., and Miller, S. E., "Analysis of a Tubular Gas Lens," *Bell System Technical Journal*, July 1964, pp. 1758–1782.

[2]Christiansen, W. H., "Gas Optics Applicable to the Free Electron Laser," *Proceedings of the 7th International Symposium on Gas Flow and Chemical Lasers*, edited by D. Schuöcker, Aug. 1988, Vol. 1031, pp. 474–479.

[3]Roshenow, W. M., and Hartnett, J. P., *Handbook of Heat Transfer*, McGraw-Hill, New York, 1973, pp. 8–85.

[4]Born, M., and Wolf, E., *Principles of Optics*, Pergamon, New York, 1970, p. 122.